



This is a repository copy of *Exergy analysis and multi-objective optimisation for energy system: a case study of a separation process in ethylene manufacturing*.

White Rose Research Online URL for this paper:
<https://eprints.whiterose.ac.uk/171223/>

Version: Accepted Version

Article:

Shen, F., Wang, M. orcid.org/0000-0001-9752-270X, Huang, L. et al. (1 more author) (2021) Exergy analysis and multi-objective optimisation for energy system: a case study of a separation process in ethylene manufacturing. *Journal of Industrial and Engineering Chemistry*, 93. pp. 394-406. ISSN 1226-086X

<https://doi.org/10.1016/j.jiec.2020.10.018>

Article available under the terms of the CC-BY-NC-ND licence
(<https://creativecommons.org/licenses/by-nc-nd/4.0/>).

Reuse

This article is distributed under the terms of the Creative Commons Attribution-NonCommercial-NoDerivs (CC BY-NC-ND) licence. This licence only allows you to download this work and share it with others as long as you credit the authors, but you can't change the article in any way or use it commercially. More information and the full terms of the licence here: <https://creativecommons.org/licenses/>

Takedown

If you consider content in White Rose Research Online to be in breach of UK law, please notify us by emailing eprints@whiterose.ac.uk including the URL of the record and the reason for the withdrawal request.



eprints@whiterose.ac.uk
<https://eprints.whiterose.ac.uk/>

Exergy analysis and multi-objective optimisation for energy system: a case study of a separation process in ethylene manufacturing

Feifei Shen^a, Meihong Wang^{a,b,*}, Lingxiang Huang^a, Feng Qian^{a,*}

^a Key Laboratory of Advanced Control and Optimisation for Chemical Processes, Ministry of Education, East China University of Science and Technology, Shanghai 200237, China

^b Department of Chemical and Biological Engineering, The University of Sheffield, Sheffield S1 3JD, United Kingdom

Abstract: In chemical industry, most processes face the challenge of high energy consumption. The approach presented in this study can reduce the energy footprint and increase efficiency. The energy system of a separation process in ethylene manufacturing is used to demonstrate the effectiveness of the approach. The chilling train system of the separation process in a typical ethylene plant consumes most cooling and provides appropriate feed for distillation columns. The steady state simulation of system was presented and the simulation results were proved accurate. The conventional exergy analysis identifies that Dephlegmator No.1 (a heat exchange and mass transfer device) has the highest exergy destruction (1401.28 kW). Based on advanced exergy analysis, Dephlegmator No.1 has the highest rate of avoidable exergy destruction (89.04 %). Finally, a multi-objective optimisation aiming to maximise system exergy efficiency and to minimise operational cost was performed and the Pareto frontier was obtained. The optimized exergy efficiency is 79.53 % (improved by 0.61 %) and the operational cost is 0.02031 yuan/kg (saved by 11.19 %). This study will guide future research to reduce energy consumption in process manufacturing.

Key words: ethylene manufacturing, separation process, steady state simulation, exergy analysis, process optimisation

1 Introduction

1.1. Background

Energy plays a vital role in industries, transportations and buildings. The petrochemical industry is responsible for about 20 % of total industrial energy consumption in China [1]. Ethylene manufacturing, one of the most important petrochemical industries, is a high energy consumption process, so study on its energy systems is of great importance.

‘Energy system’ can be considered as one system which can transform one type of energy to another or transfer energy to other places [2]. The energy systems in ethylene manufacturing have been studied by many researchers. Zhao and You [3] developed an mixed integer nonlinear programming model to optimize the industrial utility systems under uncertainty using a Dirichlet process mixture model. Shen et al. [4] modelled and optimized the energy system considering four types of energy consumption (fuel, steam, electricity and water) and obtained 14.42 % total energy consumption reduction in spring–autumn and 13.92 % in summer. In a further study, a generalized intersection kernel support vector clustering is employed to construct the uncertainty set and the robust optimisation results show that the proposed method yielded a trade-off between energy cost and robustness [5].

In addition to the utility system, the chilling train and demethanization process in ethylene manufacturing consumes large quantity of cooling and there is huge energy saving potential of this process. Chilling train system in a typical ethylene plant consists of several multi-stream plate-fin heat exchangers. The chilling train system is used to freeze the dry cracked gas and separate methane and hydrogen from heavier components such as ethane and ethylene. It is the coldest section in the ethylene manufacturing, in which the temperature can be as low as -160 °C. On the other hand, it

provides the demethanization section with suitable feed streams. The chilling train system accounts for up to 50 % cooling consumption of the ethylene production process, where refrigerants mainly include ethylene and propylene [6].

As the coldest part of ethylene plants, the chilling train system consumes large quantities of refrigerants and should improve in order to increase energy efficiency of the whole ethylene production process. There were few studies on the conventional chilling train system, where separated flashes and multi-stream heat exchangers are employed as shown in Fig.1. The charge gas from depropanizer is first cooled by CB4 and CB5, and separated in FLS1. The liquid from the bottom of FLS1 is sent to demethanizer and the vapour is further refrigerated in CB6 and separated in FLS2. In the conventional chilling train system using partial condensing technology, the charge gas is chilled to -120 °C in FLS3 and the hydrogen-rich stream is separated from heavier components (methane, ethylene, ethane and propane) through multiple cooling and separation in several units. Zhang et al. [7] performed a multi-objective optimisation on the traditional chilling train system, developing a mixed integer nonlinear programming model to optimize its design and operating conditions. Xu et al. [8] sought for higher thermal efficiency and lower costs in refrigeration system of ethylene plants by synthesis of mixed refrigerants system.

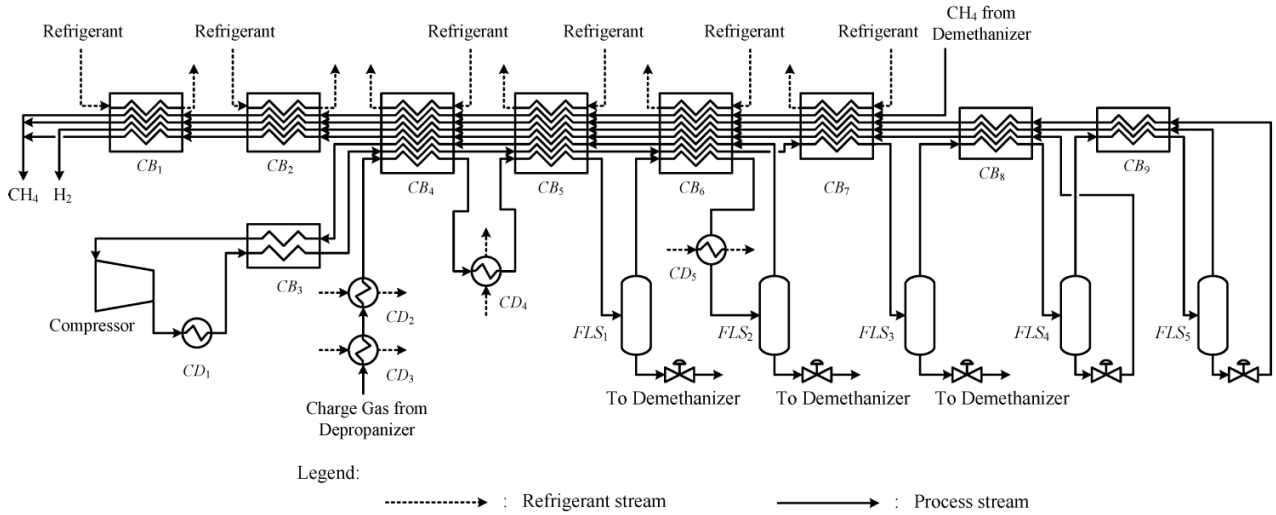


Fig.1. Diagram of conventional chilling train system using partial condensing technology [7]

In the chilling train and demethanization process with advanced recovery system (ARS), conventional partial condensation processes are replaced by the dephlegmators. In a dephlegmator, the vapor-liquid separation and heat exchange processes are combined into one unit. As shown in Fig.2, the feed vapor flows upward and heat is taken by indirect heat exchange [9]. Some vapor is condensed and the formed liquid flows downward. More volatile components in the liquid are revapourized to achieve phase equilibrium, which enhances the separation and heat exchange processes. Application of dephlegmator technology can improve ethylene recovery and simplify the process [9]. However, the introduction of dephlegmators leads to complexity in the simulation of the system. In literature, the dephlegmator has been simulated using a separation column with user-specified heat removal from each stage of the column, and obtained good agreement with pilot test results [10]. However, neglect of temperature between main streams and refrigerants in dephlegmators may result in temperature cross after optimisation, which is impossible in practice. Although the dephlegmator was simulated [10] and applied [11] in some researches, there is no publication on the simulation, exergy analysis and optimisation of the ARS chilling train system for

ethylene manufacturing.

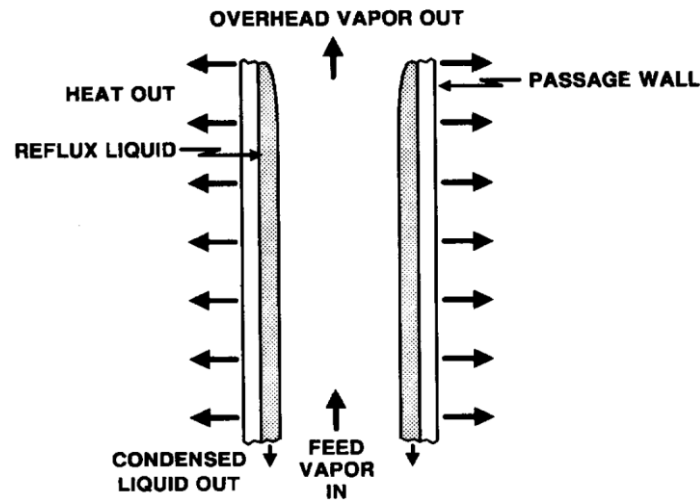


Fig.2. Dephlegmator concept [9]

1.2. Literature review

Through exergy analysis, the energy efficiency in a system can be evaluated and degradation of exergy can be located [12]. Exergy analysis has been used to find the units with highest and lowest exergy destruction. Olaleye et al. [13] performed exergy analysis of coal-fired supercritical power plant with CO₂ capture not only to identify the units with highest exergy destruction but also to compare four different CO₂ capture configurations. In their further study, qualitative potential for improvement of exergy efficiency of the post-combustion CO₂ capture components was obtained [14]. Lin and Rochelle [15] employed exergy analysis to quantify the inefficiencies of the conventional stripper in CO₂ capture and proposed an advanced flash stripper design. Bechtel et al. [16] applied exergy analysis in novel process development for efficient recycling of chlorine by gas phase electrolysis of hydrogen chloride. Elhelw et al. [17] identified the units with highest and lowest exergy destruction of steam power plant at two different operation loads and studied the relationship between operating conditions and system efficiency. Yan et al. [18] optimized a crude oil distillation plant based on exergy analysis aiming at minimizing total exergy loss. Malik et al. [19] compared three

designs of a solar desalination plant for Karachi Pakistan and identified the most recommended one based on exergy analysis. Wang et al. [20] investigated the a heavy duty truck engine running compression ignition by energy and exergy analysis and identified the irreversibility sources. Ma et al. [21] studied the impact of key operating variables on the exergy loss of the diesel methanol dual fuel engine and proposed suggestions on efficiency improvement based on the results.

Exergy analysis of ethylene manufacturing has been performed in several studies. Fabrega et al. [22] calculated exergy losses in the ethylene and propylene refrigeration cycles, and reduced 13 % of the total exergy losses by applying new operational conditions. Ghannadzadeh and Sadeqzadeh [23] performed exergy diagnosis of an ethylene production process not only to identify low efficiency units but also to provide advice for improvement based on the main units irreversibility. Jahromi et al. [24] applied an exergy analysis to evaluate the performance of distillation columns in ethylene production. Yuan et al. [25] analysed thermodynamic inefficiency for each component and assessed energy saving potential of an industrial steam cracking furnace through exergy analysis.

Exergy analysis is also applied to identify the unit with the highest percent of exergy destruction in refrigeration systems [26]. Joybari and Haghighat [27] suggested the cooling tower of single effect absorption refrigeration systems should be modified with lower cooling water mass flow rate and higher cooling water temperature according to the exergy analysis results. Wu et al. [28] performed exergy and economic analysis to illustrate the system performance of proposed hybrid source heat pump system. Sun et al. [29] utilized exergy analysis to determine the most effective refrigerants combination in cascade refrigeration systems. Chen et al. [30] calculated the exergy losses in each unit and the comparison results showed that the heat transfer areas of units should be improved. Razmi et al. [31] found the pressure regulating valve and the air turbine had the highest irreversibility in the

studied cogeneration system. However, a thorough exergy analysis of the ARS chilling train system in ethylene plants is lack.

Through the conventional exergy analysis, exergy destruction and efficiency of units can be calculated. Normally, improvements are focused on these units with high exergy destruction and low efficiency [32]. However, part of the exergy destruction may be unavoidable due to technical limitations and exogenous because of irreversibility in other units [33]. Advanced exergy analysis, concentrating on evaluating each component and the interactions with other components, has been applied in many recent researches on energy systems. Wei et al. [34] calculated avoidable/unavoidable exergy destruction of distillation columns to identify the energy saving potential. Vučković et al. [35] split exergy destruction into avoidable and unavoidable parts to identify the real thermodynamic improvement potential of the energy supply system of an industrial rubber plant. Mehrpooya et al. [36] calculated the real avoidable exergy destruction portion of a refrigeration cycle with the aid of advanced exergy analysis. Penkuhn and Tsatsaronis [37] employed conventional and advanced exergy analysis to compare the performance of two ammonia synthesis loop configurations. Mehdizadeh-Fard et al. [38] proposed the pinch technology concept combined with advanced exergy analysis (CPEA) for efficient energy saving of a heat exchanger network. Mohammadi et al. [39] determined the priority order of components for overall system improving of a recompression supercritical CO₂ cycle. In summary, advanced exergy analysis has superiority in finding inefficient components and real potential for thermodynamic improvements comparing to the conventional energy analysis, which is an important thermodynamic tool of process energy saving study [40].

In addition to system exergy efficiency, the economic performance of the system is also important to the industrial decision makers. However, lots of studies show that there is a conflict between the

system exergy efficiency and operational cost [41]. Multi-objective optimisation is proven to be efficient in obtaining a trade-off between the economic and exergetic objectives [42]. Kaviri et al. [43] performed the multi-objective optimization aiming at maximizing exergy efficiency and minimizing total cost of a combined cycle power plant using the genetic algorithm approach. Somma et al. [44] formulated a multi-objective linear problem and obtained the Pareto frontier to balance total annual cost and overall exergy efficiency of distributed energy systems. Qin et al. [45] employed Particle Swarm Optimization (PSO) to solve the global optimal solution of the integrated energy systems planning with electricity, heat and gas.

1.3. Motivation and novel contributions of this study

As reported in literature [7], optimisation of the chilling train system is very important to improve total efficiency. However, according to the previous studies reviewed in Section 1.2, there is no report of simulation and optimisation on the ARS chilling train system. Besides, exergy analysis can provide more significant guidance on improvement of the chilling train system in terms of exergy destruction and exergy efficiency. The aim of this study is to perform steady state simulation, exergy analysis and multi-objective process optimisation of the ARS chilling train system in ethylene plants.

The novel contributions of this study include: (1) Steady state simulation of the ARS chilling train system in ethylene plants using Aspen Plus[®] is performed and the model validation results are proved to be accurate; (2) Exergy analysis is applied to analyse thermodynamic irreversibility for each unit; (3) The avoidable/unavoidable exergy destructions of the units are calculated to analyse the energy saving potential, where a novel method is proposed to calculate the avoidable/unavoidable of the dephlegmators; (4) Exergy diagnosis is employed to analyse energy saving strategies for each unit; (5) Multi-objective process optimisation aiming at maximizing exergy efficiency and minimizing

operational cost is presented.

2. Steady state simulation of the ARS chilling train system

2.1. Process description

The chilling train system operates under the lowest temperature in the ethylene plant. It is composed of a series of heat exchangers, which cool the dry cracked gas to separate the methane-rich stream and produce a high-purity hydrogen-rich vapor. It also provides the feed with suitable temperature and composition for the demethanization section. The demethanization section provides part of the process refrigerants for the chilling train system and separates methane from other heavier components. The chilling train system and demethanization section are generally coupled together with the main function of separating hydrogen and methane from other heavy components. The main refrigerant consumed in the process is ethylene at different temperature levels. The ARS chilling train system, applying dephlegmators instead of conventional partial condensation processes, has high hydrocarbon recovery, low energy consumption, simplicity of operation, and modest capital investment [9]. General representation of the energy system is shown in Fig.3. The main units of this process are described in Table 1. The conditions of main inlet streams including Stream 101 (cracked gas from upstream), Stream 107 (recycle ethane from ethylene splitter) and Stream 110 (high component liquid from high pressure depropanizer condenser) are presented in Table 2. These conditions and descriptions are all based on a real ethylene plant in China.

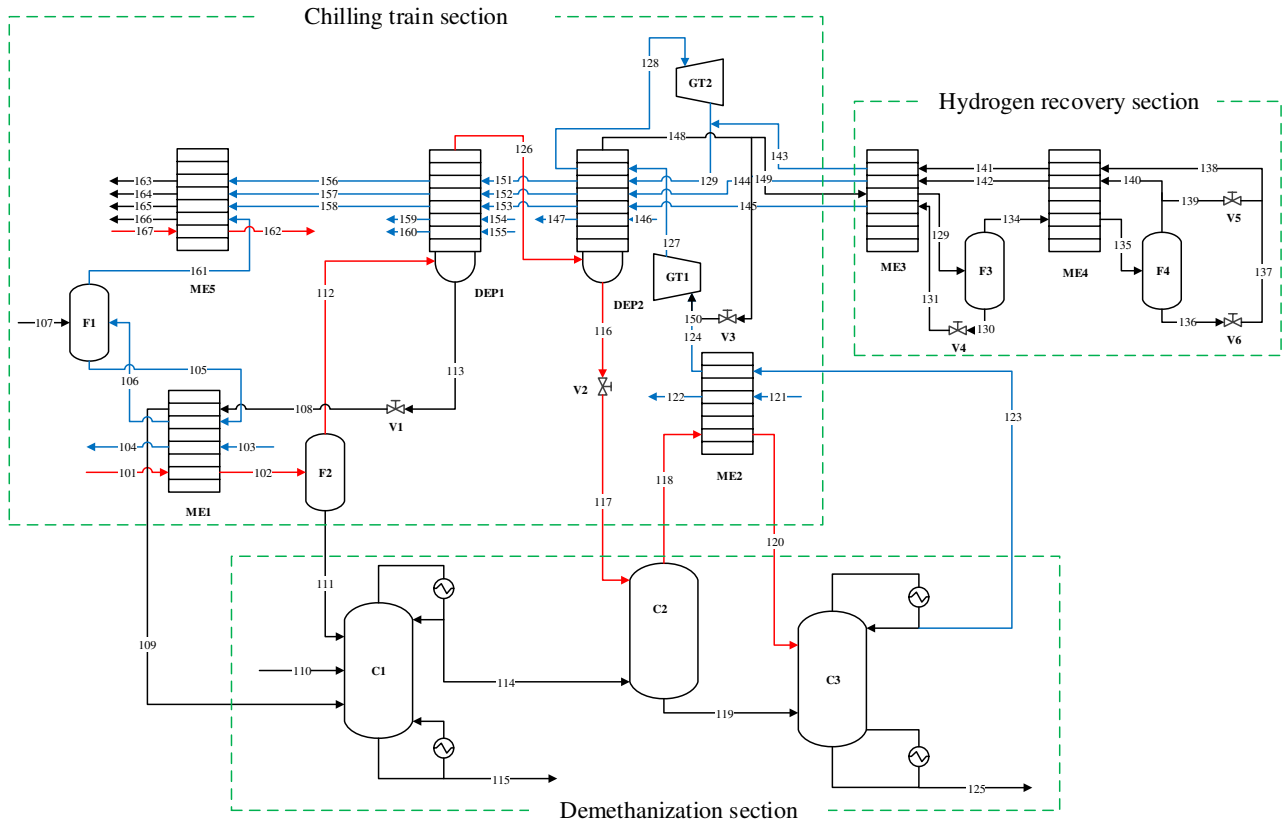


Fig.3. General representation of the ARS chilling train and demethanization process

(The red lines represent main hot streams and the blue lines represent main cold streams) [6]

Table 1. Types and descriptions of the units of the chilling train and demethanization process [6]

Unit	Type	Description
DEP1	Dephlegmator	Dephlegmator No.1
DEP2	Dephlegmator	Dephlegmator No.2
ME1	Multi-stream heat exchanger	Prefractionator feed chiller
ME2	Multi-stream heat exchanger	Demethanizer feed chiller
ME3	Multi-stream heat exchanger	Hydrogen core exchanger No.1
ME4	Multi-stream heat exchanger	Hydrogen core exchanger No.2
ME5	Multi-stream heat exchanger	Propylene refrigerant subcooler
F1	Flash	Demethanizer bottom flash pot
F2	Flash	Demethanizer prefractionator feed drum
F3	Flash	Hydrogen drum No.1
F4	Flash	Hydrogen drum No.2
C1	Distillation column	Demethanizer prefractionator
C2	Multi-level flash column	Demethanizer feed rectifier
C3	Distillation column	Demethanizer
GT1	Expander	Tail gas expander A
GT2	Expander	Tail gas expander B
V1	Valve	Throttle valve No.1

V2	Valve	Throttle valve No.2
V3	Valve	Throttle valve No.3
V4	Valve	Throttle valve No.4
V5	Valve	Throttle valve No.5
V6	Valve	Throttle valve No.6

Table 2. Conditions of the main inlet streams of the system

	Stream 101	Stream 107	Stream 110
Temperature (°C)	-17.6	-38.60	-18.01
Pressure (MPa)	3.44	0.83	3.13
Mole Flow (kmol/h)	5071.9	191.7	198.86
Component composition (mole fraction)			
Hydrogen	0.2095	0	0.0087
Carbon monoxide	0.0003	0	0
Methane	0.3406	0	0.1016
Ethylene	0.3219	0.0050	0.3787
Ethane	0.0517	0.9821	0.0877
Methyl-acetylene	0.0002	0	0.0022
Propadiene	0.0005	0	0.0040
Propylene	0.0668	0.0125	0.3566
Propane	0.0078	0	0.0493
1-butene	0.0002	0	0.0033
Isobutylene	0.0002	0	0.0039
Isobutane	0.0001	0	0.0013
N-butane	0.0001	0	0.0011

The dried cracked gas (Stream 101) from the five-level compression section is chilled by recycled ethane (Stream 105), propylene refrigerant (Stream 103) and DEP1 bottom liquid (Stream 108) in ME1. The dephlegmator is a multi-stream plate-fin heat exchanger where one stream is separated into vapor and liquid phases at the same time. In the main channel, condensed liquid flows downward, counter flows with the upward flowing vapor. The vapor product of F2 is chilled and fractionated in DEP1. The cold streams in DEP1 are ethylene at -60 °C (Stream 155), ethylene at -80 °C (Stream 154), cold tail gas (Stream 151), methane-rich gas (Stream 153) and hydrogen-rich gas (Stream 152). The main vapor stream of DEP1 is further chilled and fractionated in DEP2 by cold tail gas from GT1 (Stream 127) and GT2 (Stream 129), cold hydrogen (Stream 144) and methane-rich gas (Stream 145)

from the hydrogen recovery section. Vapor from the top of DEP2 is split into two streams and then flow to the hydrogen recovery section and to GT1, respectively.

The demethanizer prefractionator (C1) has three feed streams, namely, F2 bottom liquid (Stream 111), low pressure depropanizer overhead liquid (Stream 110) and DEP1 bottom liquid (Stream 109), and they are separated into a C₃-free overhead vapor and a methane-free bottom liquid. The column is reboiled by propylene refrigerant and partly condensed by ethylene refrigerant at -100 °C.

The hydrogen recovery section separates methane from the mixture. The vapor of DEP2 is split into two streams, of which one stream is cooled in ME3 before it enters F3 and the other is sent to GT1 as cold tail gas. The liquid of F3 flows back to ME3 and the vapor is further cooled in ME4 and separated in F4. The methane-rich liquid from the bottom (Stream 136) and the hydrogen-rich vapor from the top (Stream 140) of F4 are used as heat exchange media in ME4.

The tail gas expander A (GT1) expands high pressure tail gas and hydrogen to produce an extremely cold refrigerant, which is used to cool the feed stream in DEP1 and DEP2. This can reduce the loss of the main product ethylene in the tail gas and reduce the refrigerant consumption. The overhead vapors of DEP2 and C3 flow to GT1 and are subsequently reheated in DEP2. After that step, it flows to GT2 for further pressure let-down. The low-pressure tail gas from GT2 is combined with the methane-rich gas from ME3 and then reheated in DEP2.

2.2. Steady state simulation and model validation

The simulation of the chilling train system is performed in Aspen Plus[®] V8.4 as shown in Fig.4 because Aspen Properties[®] has a comprehensive physical property database. This system mainly involves hydrocarbons and hydrogen, so the global thermodynamic method selected is the SRK (Soave-Redlich-Kwong), which is for weakly polar and non-polar real gases. For the units with

methane-rich and hydrogen-rich streams, the RK-ASPEN, which fits the simulation of mixture of polar components and hydrocarbons and also suits the light gases simulation under medium and high pressure, is selected as suggested in Aspen Plus[®] help files [46].

Table 3. Thermodynamic properties in each point [46]

Thermodynamic properties	Unit
SRK	DEP1, DEP2, ME1, ME2, ME5, C1, C2, C3, F1, F2
RK-ASPEN	ME3, ME4, F3, F4, GT1, GT2

Considering that there are multi-level heat exchange and gas-liquid separation processes simultaneously in dephlegmators, here a ‘Radfrac’ model block without condensers and reboilers is selected to simulate the complex process. Later on, the five-stage cooling process is calculated in ‘Heater’ models respectively with an energy flow to the ‘Radfrac’ as cooling supply. For other units, there are corresponding built-in models (ME-MHeatX, F-Flash2, C-Radfrac, V-Valve, GT-Compr). Here these models are assumed to be perfect theoretical models without exergy destruction. As in the large-scale ethylene plant, the heat loss is relatively small compared to the heat transfer, the heat loss in the real plant is not considered.

Such a system with complex recycle loops is difficult to converge in Aspen Plus[®]. To handle this problem, design specifications of sensitive stage temperature with varying reflux ratio and reboiler duty were set for distillation columns. In addition, Streams 113, 114, 116 and 126 were given initial values according to industrial data. Certain tearing streams are also added for the convergence of large system based on the process analysis.

Data for the model validation were collected from a real ethylene plant in China and reconciled before use, so the impact of measurement uncertainties can be ignored. Model predictions and real plant data together with absolute and relative errors are shown in Table 4. For most temperatures

listed, absolute errors are less than 5 °C and absolute error of mole fraction of ethylene in bottom liquid of C3 is as low as 0.001. Relative errors of bottom streams flowrates of DEP1, DEP2 and C1 are all less than 5 %. For the temperature of the bottom stream of C1, the temperature and the key mole fraction of the bottom stream of C3, the absolute values of their plant data are small and the absolute errors meet the industrial requirement.

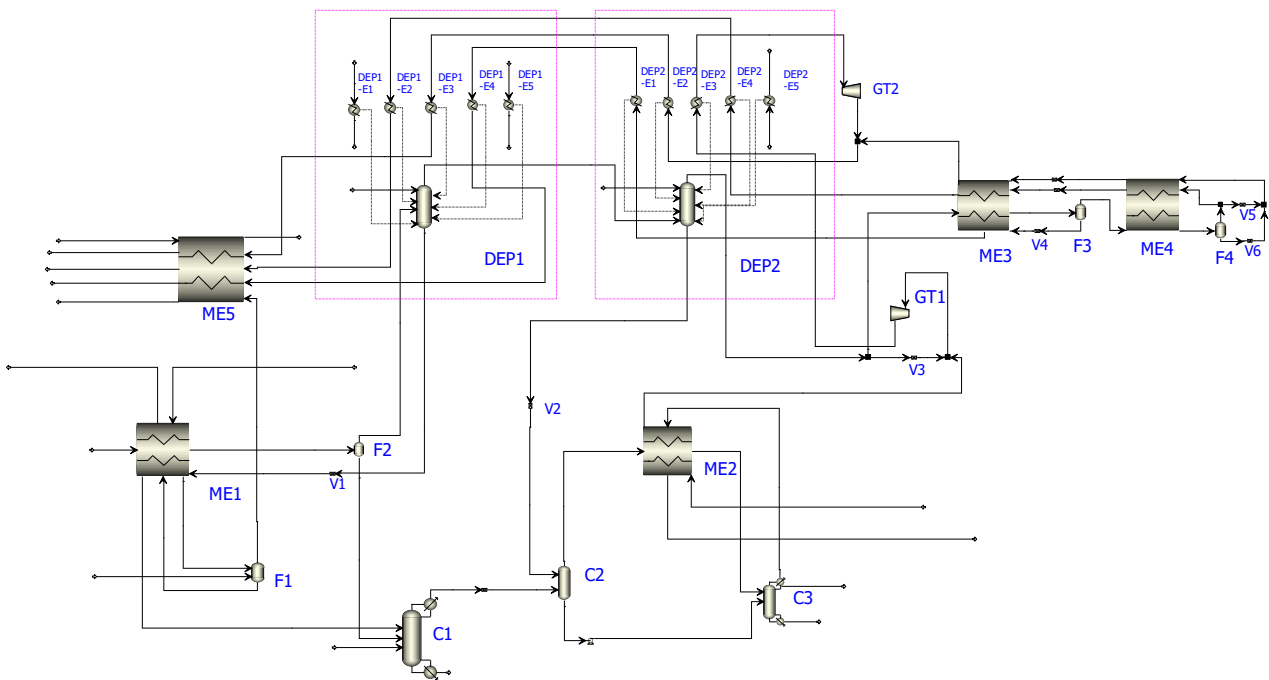


Fig.4. Aspen Plus® simulation flowsheet of the ARS chilling train and demethanization system (The red dashed boxes represent the models of DEP1 and DEP2 respectively)

Table 4. Steady state simulation results of the ARS chilling train and demethanization system

Unit	Variable	Plant data	Model prediction	Absolute error	Relative error (%)
DEP1	T_{DEP1}^{ovhd} (°C)	-82.20	-82.24	-0.04	0.05
	F_{DEP1}^{bm} (kg/h)	3.33×10^4	3.49×10^4	1.52×10^3	4.56
	T_{DEP1}^{bm} (°C)	-47.12	-44.91	2.21	-4.69
DEP2	T_{DEP2}^{ovhd} (°C)	-114.64	-113.00	1.64	-1.43

	F_{DEP2}^{btm} (kg/h)	9310.00	9440.00	130.00	1.40
	T_{DEP2}^{btm} (°C)	-83.01	-83.40	-0.39	0.47
C1	T_{C1}^{ovhd} (°C)	-42.20	-42.00	0.20	-0.47
	T_{C1}^{btm} (°C)	4.85	5.50	0.65	13.40
	F_{C1}^{btm} (kg/h)	5.74×10^4	5.93×10^4	1.87×10^3	3.25
	T_{C1}^{sen} (°C)	-6.82	-6.80	0.02	-0.29
C3	T_{C3}^{ovhd} (°C)	-96.60	-96.50	0.10	-0.10
	T_{C3}^{btm} (°C)	-10.60	-10.00	0.60	-5.66
	T_{C3}^{sen} (°C)	-26.70	-26.00	0.70	-2.62
	$x_{C3}^{btm,ethylene}$	0.012	0.011	0.001	-8.33
ME3	$T_{ME3}^{in,methane}$ (°C)	-163.50	-169.00	-5.50	3.36
	$T_{ME3}^{out,cracked gas}$ (°C)	-157.92	-157.00	0.92	-0.58
ME4	$T_{ME4}^{in,methane}$ (°C)	-144.29	-141.90	2.39	-1.66
	$T_{ME4}^{out,cracked gas}$ (°C)	-141.70	-141.80	-0.10	0.07

3. Exergy analysis

3.1. Conventional exergy analysis method

The exergy analysis can evaluate energy saving potential quantitatively and qualitatively. Exergy, as defined in literature [47], is the maximum work that one system can obtain when reaches a state of reversible thermodynamic equilibrium with the environment. In a steady-state system, exergy of the process stream contains physical exergy and chemical exergy.

Physical exergy is defined as the maximum work obtainable when one system is brought from process state to the environmental state (T_0, P_0) through a physical process [48]. The physical exergy (E^{ph}) is given in Eq. (1), where H and S are the enthalpy and entropy of the system, respectively.

$$E^{ph} = H(T, P, z) - H(T_0, P_0, z) - T_0 (S(T, P, z) - S(T_0, P_0, z)) \quad (1)$$

Chemical exergy is defined as the maximum work that one system can obtain when it is brought from environmental state to the standard dead state [48]. The chemical exergy (E^{ch}) is expressed by Eq. (2) including exergy caused by chemical reaction and concentration change. Here x_i is the mole fraction of component i and e_i^0 is the molar standard chemical exergy which is given in Eq. (3).

$$E^{ch} = \sum_{i=1}^n x_i (e_i^0 + RT \ln x_i) \quad (2)$$

$$e_i^0 = \Delta G_f^0 + \sum_{j=1}^{n_i} n_{i,j} e_j^0 \quad (3)$$

In the exergy analysis, the system exergy balance can be expressed as Eqs. (4) to (6), where $E_{F,tot}$ is the exergy of total feed streams of the system, $E_{P,tot}$ is the exergy of the total product streams of the system, $E_{D,tot}$ is the total exergy destruction of the system, $E_{L,tot}$ is the total exergy loss of the system and $E_{D,k}$ is exergy destruction of k^{th} unit. Here the system boundaries for all exergy balances are at the temperature T_0 and pressure P_0 of the reference environment ($T_0 = 25$ °C and $P_0 = 101.325$ kPa) [49]. Therefore, there is no heat loss associated with heat transfer to the environment [50]. Here the boundary is the overall system, so we assume exergy losses appear only at the level of the overall system. The following equations are generally used for the exergetic evaluation of the overall system and an individual unit [51], [52].

$$E_{F,tot} = E_{P,tot} + E_{D,tot} + E_{L,tot} \quad (4)$$

$$E_{D,tot} = \sum_{k=1}^K E_{D,k} \quad (5)$$

$$\mathcal{E}_{tot} = \frac{E_{P,tot}}{E_{F,tot}} \quad (6)$$

$$E_{D,k} = E_{F,k} - E_{P,k} \quad (7)$$

$$\mathcal{E}_k = \frac{E_{P,k}}{E_{F,k}} \quad (8)$$

For the dephlegmators and multi-stream heat exchangers, there is only a physical change and the

chemical exergy does not change since the chemical composition of the refrigerant streams do not change during the heating or cooling process [48]. As the chemical exergy is much larger than the physical exergy for these streams, the exergy destruction is small relative to the feed exergy and the exergy efficiency is close to 1. Therefore, the exergy destruction of heat exchange units is defined as the difference between the exergy provided by cold streams and that consumed by the hot streams in Eq. (9) and the exergy efficiency is calculated with Eq. (10) [52].

$$E_{D,k} = (E_{F,k}^{cold} - E_{P,k}^{cold}) - (E_{F,k}^{hot} - E_{P,k}^{hot}) \quad (9)$$

$$\varepsilon_k = \frac{E_{F,k}^{hot} - E_{P,k}^{hot}}{E_{P,k}^{cold} - E_{F,k}^{cold}} \quad (10)$$

3.2. Location of exergy destruction

Through the conventional exergy analysis, the total system exergy destruction is 7621.60 kW and exergy efficiency is 78.92 %. The exergy destruction of different units is mapped as shown in Fig.5. It shows that DEP1, DEP2, C1 and C3 have the highest irreversibility, followed by F2 and F3. On most trays of the distillation column, the mass transfer driving forces are large, resulting in large irreversibility [23]. In dephlegmators, the conditions are the same as that in columns, which means high exergy destruction happens in dephlegmators, too. Expanders have relative low exergy destruction and most valves have low exergy destruction that is less than 100 kW expect V5.

Detailed exergy destruction of units is shown in Fig.6. DEP1 has the highest exergy destruction which is up to 1401.28 kW. C1, following DEP1, has 1088.47 kW exergy destroyed. Exergy destruction of multi-stream heat exchangers are close, which is in the range of 85 to 320 kW. F1 operates at lower pressure, leading to lower exergy destruction (6.01 kW) than F2 (448.33 kW), F3 (424.49 kW) and F4 (132.00 kW). C2 has much lower exergy destruction (138.64 kW) than C1 (1088.47 kW) and C3 (790.81 kW) because it is actually a multi-level flash. V1 (0.90 kW), V2 (1.94

kW) and V6 (10.56 kW), unlike V3 (28.31 kW) and V5 (479.81 kW), are used to balance the pressure instead of reducing pressure, which means lower irreversibility compared to V3 and V5.

As presented in Fig.7, exergy efficiencies of most units of the energy system are higher than 80 %. The least exergy efficient unit is ME5 (38.58 %), which only makes use of sensible heat. Heat exchangers using latent heat (ME1, ME2, ME3 and ME4) have higher exergy efficiency. Most valves have high exergy efficiencies that are close to 1, however, large pressure drop in V5 (2.87 MPa) leads to low efficiency (58.22 %). Dephlegmators are not only heat exchangers but also have mass transfer inside. Therefore DEP1 and DEP2 have low exergy efficiencies, 40.34 % and 51.12 % respectively.

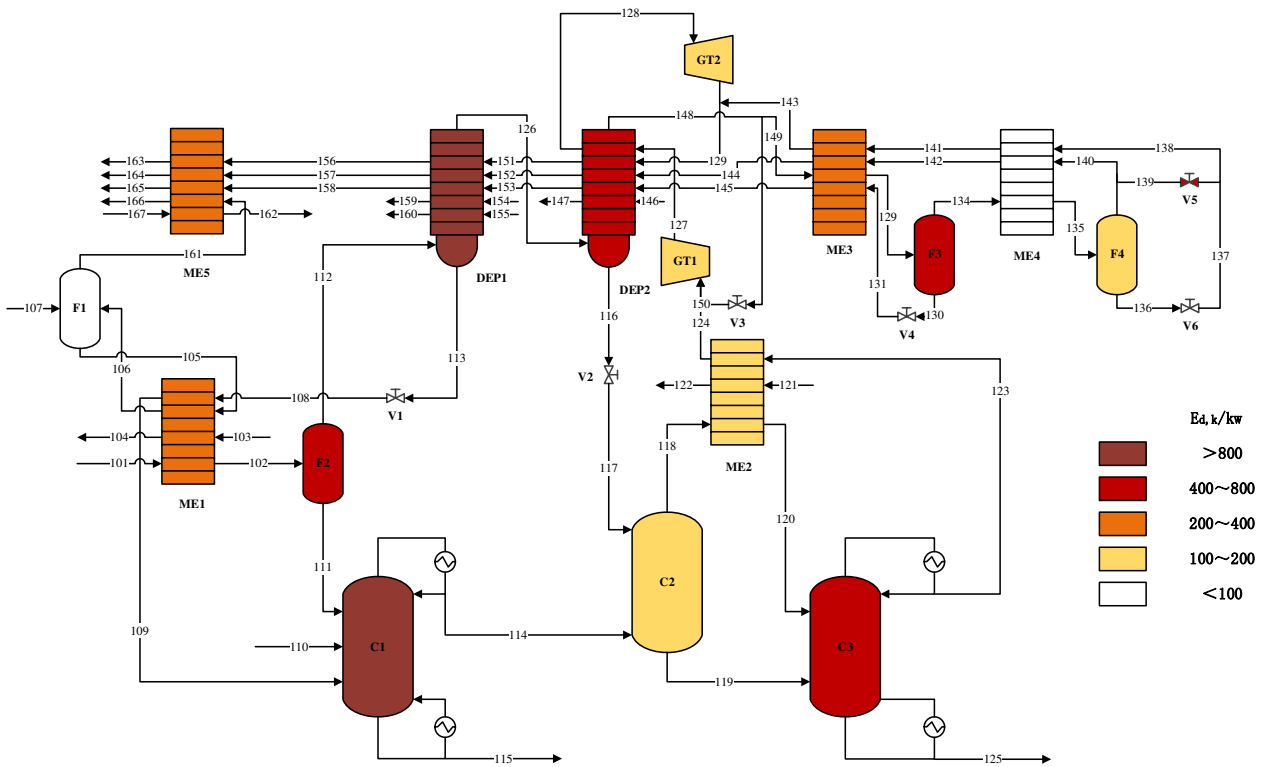


Fig.5. Exergy destruction map of the chilling train and demethanization process

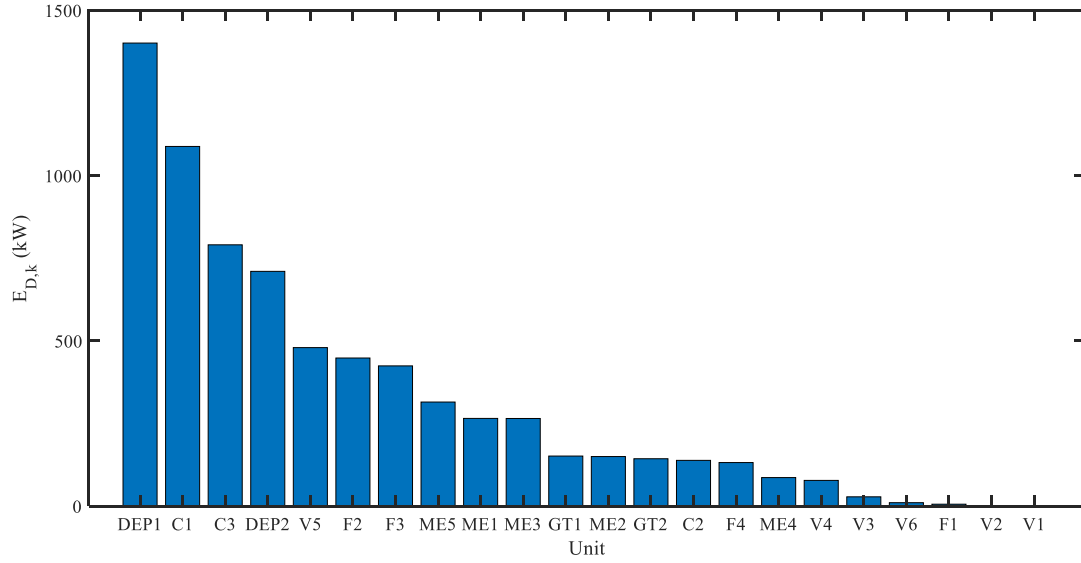


Fig.6. Units exergy destruction of the chilling train and demethanization process

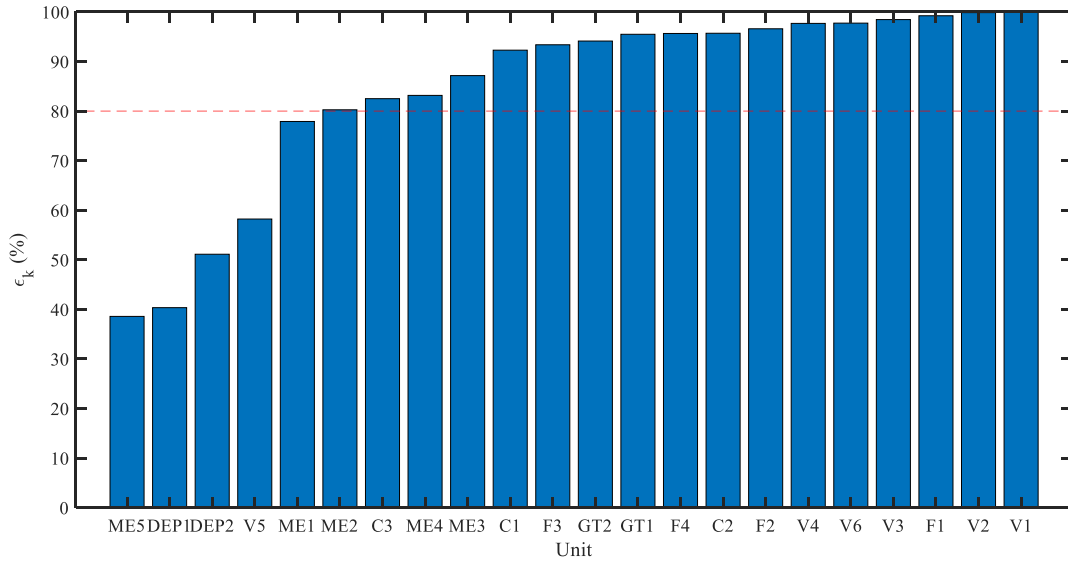


Fig.7. Units exergy efficiency of the chilling train and demethanization process

3.3. Avoidable/unavoidable exergy destruction analysis

Through advanced exergy analysis, the exergy destruction can be split into unavoidable and avoidable exergy destruction [53]. The exergy destruction can be defined as Eq (11) and unavoidable exergy destruction can be calculated based on the standard unit of the same type as Eq (12).

$$E_{D,k} = E_{D,k}^{UN} + E_{D,k}^{AV}, \quad \forall k \in K \quad (11)$$

$$E_{D,k}^{UN} = E_{P,k} (E_D / E_P)_0^{UN}, \quad \forall k \in K \quad (12)$$

To calculate unavoidable part of units exergy destruction, the unavoidable operating conditions of units in the energy system should be determined firstly. For the multi-stream heat exchanger, flash and expander, the unavoidable operating conditions are set as shown in Table 5, namely, minimum temperature approach equals to 0.5 °C and pressure drop equals to zero for MEs [54], isentropic efficiency equals to 0.9 for flashes and GTs [55]. The unavoidable condition of distillation columns is operating under minimum reflux ratio and the pressure drop on the feed stage equals zero [34], where the minimum reflux ratio can be calculated according to Underwood's method as Eq (13) and Eq (14).

$$\sum_i^n \frac{\alpha_i x_{feed,i}}{\alpha_i - \theta} = 1 - q \quad (13)$$

$$R_{min} = \sum_i^n \frac{\alpha_i x_{ovhd,i}}{\alpha_i - \theta} - 1 \quad (14)$$

For the dephlegmator, there is no literature about its unavoidable condition. As the dephlegmator is a multi-stream heat exchanger with vapor-liquid separation, its unavoidable condition is set for the first time according to that of the multi-stream heat exchanger (minimum temperature approach equals to 0.5 °C and pressure drop equals to zero).

Table 5. Unavoidable operating conditions of units in the energy system.

Type of unit	Unavoidable condition
Dephlegmator	$\Delta T_{app}=0.5$ °C, $\Delta P=0$ kPa
Multi-stream heat exchanger	$\Delta T_{app}=0.5$ °C, $\Delta P=0$ kPa
Flash	$\eta_{is}=0.9$
Distillation column	$R=R_{min}$, $\Delta P_{feed}=0$ kPa
Expander	$\eta_{is}=0.9$

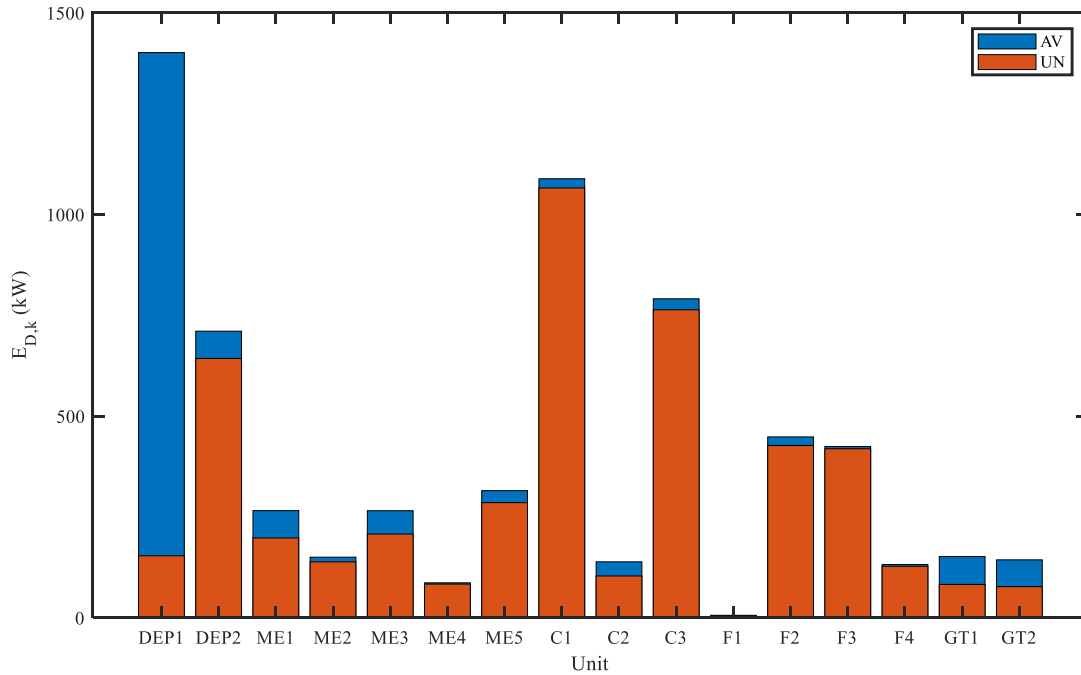


Fig.8. Units avoidable/unavoidable exergy destruction of the chilling train and demethanization process

The unavoidable and avoidable exergy destruction of units of the energy system are presented in Table 6 and Fig.8. Although the chilling train process with advanced recovery system is a well-developed process, there is still opportunity for system improvement. Dephlegmator No.1 has the highest rate of avoidable exergy destruction, which is 89.04 %. Although the DEPs have similar equipment structure, the temperature difference between hot and cold streams in DEP2 is much lower than that in DEP1, leading to much less avoidable exergy destruction than DEP1. Compared with other three MEs, ME2 and ME4 are better designed with less than 10 % avoidable exergy destruction. The reason is ME2 and ME4 have low temperature difference between hot and cold streams. For distillation columns (C1 and C3), most exergy destruction is due to the concentration gradient along the unit, which is hard to reduce by adjusting operational conditions. So little exergy destruction, 2.10 % of C1 and 3.45 % of C3 is avoidable, which can be achieved by reducing pressure drop along stages. Since C2 has no condensers and reboilers, it is actually a multi-stage flash column which has

more avoidable exergy destruction than C1 and C3. Among the flashes, F1 has the lowest isentropic efficiency, which means more avoidable exergy destruction. As the pressure drop of both expanders (GT1 and GT2) are high, about half of their exergy destruction is avoidable.

Table 6. Unavoidable and avoidable exergy destruction of units of the energy system

Unit	$E_{D,k}^{UN}$ (kW)	$E_{D,k}^{AV}$ (kW)	$E_{D,k}^{UN}$ (%)	$E_{D,k}^{AV}$ (%)
DEP1	153.55	1247.73	10.96	89.04
DEP2	642.93	67.60	90.49	9.51
ME1	197.71	67.87	74.45	25.55
ME2	138.56	11.62	92.26	7.74
ME3	207.48	57.89	78.19	21.81
ME4	83.47	3.07	96.45	3.55
ME5	285.31	29.81	90.54	9.46
C1	1065.59	22.88	97.90	2.10
C2	103.57	35.07	74.70	25.30
C3	763.53	27.28	96.55	3.45
F1	5.06	0.95	84.19	15.81
F2	427.01	21.32	95.24	4.76
F3	418.96	5.53	98.70	1.30
F4	127.54	4.46	96.62	3.38
GT1	82.67	69.00	54.51	45.49
GT2	77.02	66.52	53.66	46.34

3.4. Exergy diagnosis

As presented in section 3.2, DEP1 accounts for the highest exergy destruction, followed by C1 and C3. The exergy diagnosis, which is based on the analysis in literature [23], is employed to find the main sources of irreversibility and propose unit improvement suggestions.

Dephlegmators: The exergy destruction in DEP1 and DEP2 attributes to the temperature difference and concentration gradient inside because the dephlegmator combines the vapor-liquid separation and heat exchange processes. As a compact heat exchange and mass transfer device, the dephlegmator is designed to reduce energy cost and also to simplify the process. However, DEP1 has large exergy destruction, which is 1401.28 kW. The dephlegmators are in the middle position of the system and the change of operational conditions may lead to system infeasibility. Despite that, the flowrate of

independently imported refrigerants can be adjusted to achieve higher exergy efficiency.

Heat exchangers: The irreversibility in heat exchangers is mainly due to the unavoidable temperature difference and pressure drop. ME5, which is the least efficient heat exchanger, has up to 8.79 °C temperature difference between hot and cold streams. In other heat exchangers, the temperature difference is about 3 °C. So the exergy destruction can be reduced by reducing the temperature difference and pressure drop.

Flashes: Generally, the phase-change-followed pressure drop brings irreversibility. As these flashes are set under isothermal and isobaric conditions, it is difficult to change the operational conditions to reduce exergy destruction.

Columns: There are three types of sources in distillation columns: (1) the temperature difference between inlet and distillate streams; (2) the pressure difference between inlet and distillate streams; (3) the concentration gradient along the unit. The exergy destruction caused by the first two reasons can be reduced by adjusting the operational conditions of the upstream units as well as adding pressure change and heat exchange units before the inlet streams flow into columns.

Expanders: The main reasons of exergy destruction in the expanders are pressure drop and temperature decrease during the expanding process. The low isentropic efficiencies and mechanical efficiencies also contribute to the irreversibility. The exergy destruction in GT1 and GT2 is 151.67 kW and 143.54 kW respectively, which may be decreased by applying more efficient units.

Valves: The exergy destruction in valves has the same source as that in expanders. V5 has the highest exergy destruction comparing to other valves because it has a pressure drop up to 2.93 MPa. This can be improved by choosing more efficient valves and using a turbine for big pressure change.

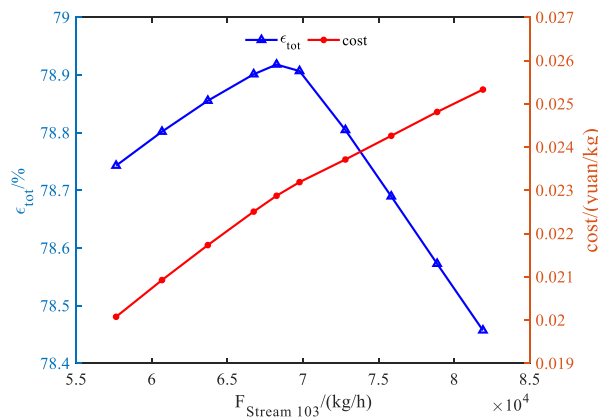
4. Process optimisation

4.1. Sensitivity analysis

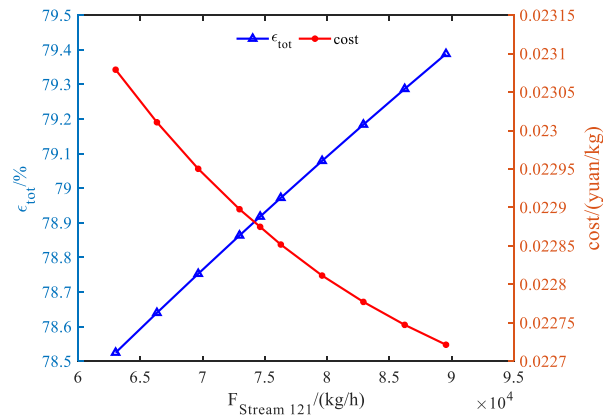
To study the effect of key variables on the exergy efficiency and operational cost of the system, the sensitivity analysis was performed. The following assumptions were made: (a) In each case, only one variable changes while others are fixed. (b) These variables are restricted in the range of 80 % to 120 % of their current values in the sensitivity analysis. Description of key variables of the system is listed in Table 7 and the sensitivity analysis results are presented from Fig.9 to Fig.11. As shown in Fig.9, with the increase of flowrate of Stream 103, the system exergy efficiency first increases and then decreases (reaches the peak at 68246 kg/h). Although more heat exchange medium imported to ME1 leads to higher operational cost, the trend for ME2 is the opposite.

Table 7. Description of key variables of the system

Stream	Heat exchange medium	Unit
103	Propylene refrigerant at -40 °C	ME1
121	Ethylene refrigerants at -80 °C	ME2
154	Ethylene refrigerants at -60 °C	DEP1
155	Ethylene refrigerants at -80 °C	DEP1
146	Ethylene refrigerants at -100 °C	DEP2



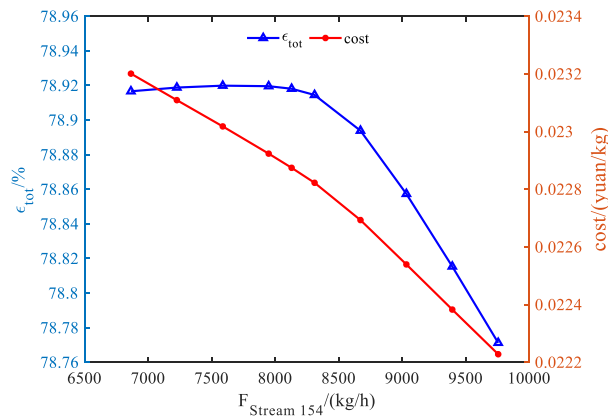
(a) Imported heat exchange medium of ME1



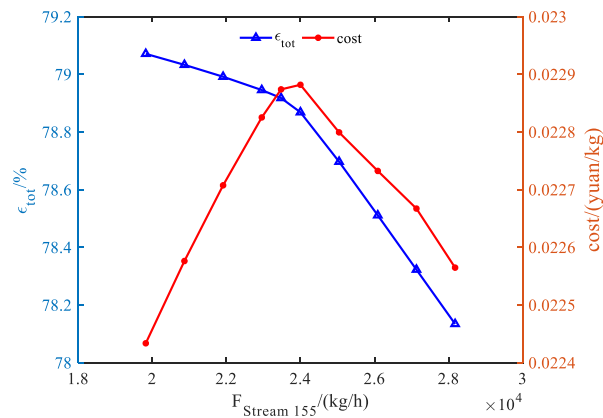
(b) Imported heat exchange medium of ME2

Fig.9. Sensitivity analysis of the flowrate of imported heat exchange medium of ME

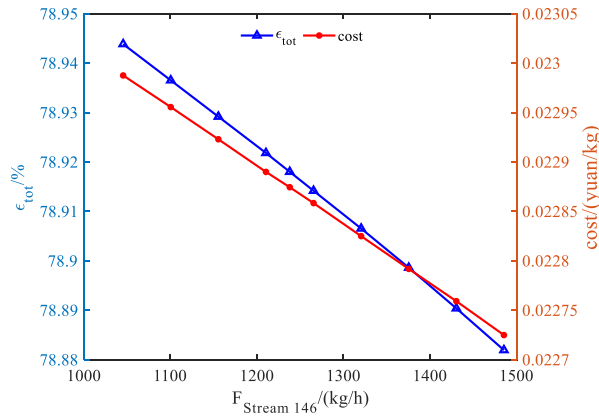
As shown in Fig.10, the flowrates of Stream 154 and Stream 146 have less influence on the system exergy efficiency comparing to that of Stream 155. Generally, more refrigerants imported to DEPs brings more irreversibility to the system while leads to less cost.



(a) Imported heat exchange medium of DEP1



(b) Imported heat exchange medium of DEP1



(c) Imported heat exchange medium of DEP2

Fig.10. Sensitivity analysis of the flowrate of imported heat exchange medium of DEP

In addition to heat exchange streams flowrates, the split fraction of Stream 149 from Stream 148 is a key variable, leading to lower system exergy efficiency and less operational cost with Stream 149 fraction increases as shown in Fig.11.

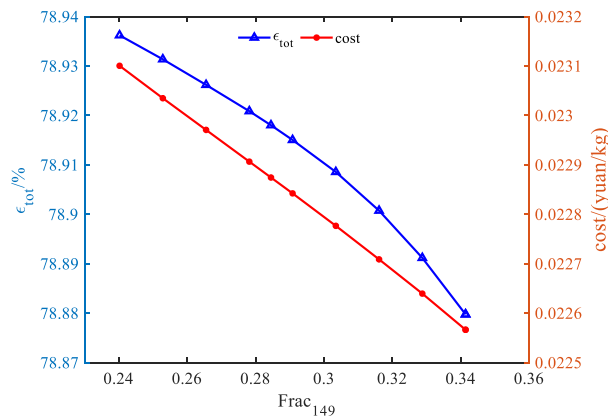


Fig.11. Sensitivity analysis of the split fraction of Stream 149 from Stream 148

4.2. Optimisation of the chilling train and demethanization system

The chilling train system accounts for most refrigerant consumption in the whole ethylene plant, so it is significant to perform operational optimisation on the system. Based on the sensitivity analysis results and feasibility consideration, flowrates of heat exchange media in ME1 (Stream 103), ME2

(Stream 121), DEP1 (Stream 154, Stream 155) and ME5 (Stream 167) and the split fraction of Stream 149 are set as decision variables, which are not only relatively convenient to manipulate but also affect the system performance a lot. As the process optimization is performed on an existing ethylene plant, only operational cost is taken into account.

The multi-objective optimisation contains two objectives: one is to minimize operational cost as in Eq.(15) and another is to maximize system exergy efficiency as in Eq. (16). To make sure the system operates normally, two kinds of constraints were applied in the formation of the optimisation problem: the temperature difference between hot process streams and refrigerants on each stage of dephlegmators constraints (Eq. (17)) and the key components mole fraction in overhead and bottom of streams of columns constraints (Eq. (18) and Eq. (19)). Here the minimum temperature difference is set to be 3 °C according to the historical industrial data and experience.

$$\min_{F_{stream103}, F_{stream121}, F_{stream154}, F_{stream155}, F_{stream167}, Frac_{149}} \quad obj_1 = \left(\omega_{ethylene}^{re} \sum_k F_{ethylene,k}^{re} + \omega_{propylene}^{re} \sum_k F_{propylene,k}^{re} \right) / F_{ethylene}^{pro} \quad (15)$$

$$\max_{F_{stream103}, F_{stream121}, F_{stream154}, F_{stream155}, F_{stream167}, Frac_{149}} \quad obj_2 = \varepsilon_{tot} \quad (16)$$

$$s.t. \quad T_{k,s}^{main} - T_{k,s}^{cold,in} > \Delta t_{min} \quad (17)$$

$$x_{i,k}^{ovhd} = x_{i,k}^{ovhd,spec} \quad (18)$$

$$x_{i,k}^{btm} = x_{i,k}^{btm,spec} \quad (19)$$

Because of the complex recycle loops and constraints in this system, the optimisation problem is hard to converge. The PSO algorithm, as a computational intelligence-based method, can efficiently solve nonlinear optimization problems when general methods fail to converge [56]. The optimisation was performed using MATLAB R2019b applying the PSO algorithm. The purpose of multi-objective optimisation is to obtain the Pareto frontier (a set of non-dominated solutions), then the decision makers can select the optimal solution according to their requirements.

The Pareto frontier of the multi-objective optimisation is shown in Fig.12. Each point on the Pareto frontier represents an optimal design, and the optimal economic and exergetic designs are as shown in this figure. At the ideal point, the two objectives simultaneously reach their best values. However, the ideal condition is actually non-existent. It should be noted that the unit quantity of exergy efficiency is much higher than that of operational cost, the distance between each point and the ideal point is calculated with the normalized values [57]. The multi-objective optimized design (0.02031, 79.53) can be determined as marked in Fig.12.

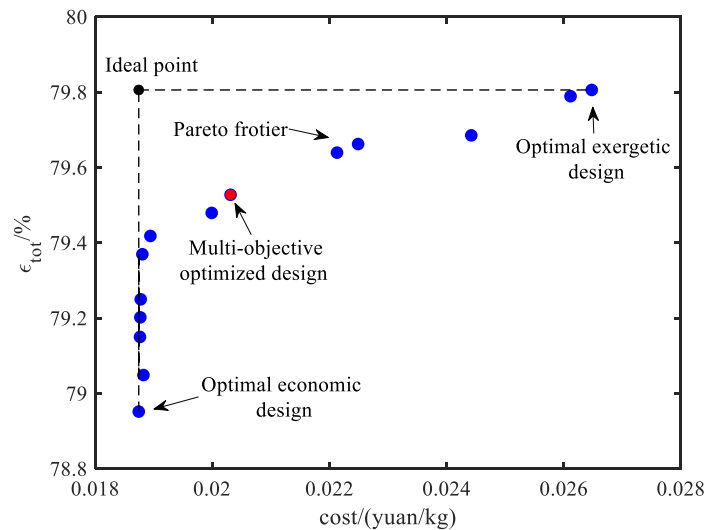


Fig.12. Pareto frontier of the multi objective optimization

The optimisation solutions of the ARS chilling train and demethanization system are as shown in Table 8. The optimal economic design is: (a) increasing $F_{\text{stream}121}$ and $F_{\text{stream}154}$; (b) decreasing $F_{\text{stream}103}$, $F_{\text{stream}155}$, $F_{\text{stream}146}$ and Frac_{149} . The minimum operational cost is 0.01874, which is reduced by 18.06 % (1.239 million yuan operational cost saving per year for a 300 kt/year ethylene plant). The exergy efficiency of this design is also slightly improved compared to the current value. The optimal exergetic design is: (a) increasing $F_{\text{stream}103}$ and $F_{\text{stream}121}$; (b) decreasing $F_{\text{stream}154}$, $F_{\text{stream}155}$, $F_{\text{stream}146}$ and Frac_{149} . The maximum exergy efficiency is 79.81 %, which is 0.89 % higher than the current

value. However, the operational cost of this design increases by 15.78 % compared to the current value, which may not be acceptable for an industrial decision maker. By (a) increasing $F_{\text{stream121}}$ and $F_{\text{stream154}}$; (b) decreasing $F_{\text{stream103}}$, $F_{\text{stream155}}$, $F_{\text{stream146}}$ and Frac_{149} , the multi-objective optimum design is obtained. The multi-objective optimized exergy efficiency is 79.53 % (improved by 0.61 %) and the operational cost is 0.02031 yuan/kg (saved by 11.19 %).

Table 8. Multi-objective optimisation results of the ARS chilling train and demethanization process

Unit	Variable	Current value	Optimal economic design	Optimal exergetic design	Multi-objective optimized design
ME1	$F_{\text{stream103}}$ (kg/h)	68246.38	57080.14	81895.54	62200.42
ME2	$F_{\text{stream121}}$ (kg/h)	74624.60	75846.14	89549.52	89549.52
DEP1	$F_{\text{stream154}}$ (kg/h)	8129.95	9308.19	6584.66	9755.94
DEP1	$F_{\text{stream155}}$ (kg/h)	23479.10	18783.28	18783.33	18783.28
DEP2	$F_{\text{stream146}}$ (kg/h)	1237.89	1183.75	990.83	990.31
	Frac_{149}	0.2845	0.2745	0.2276	0.2565
	ϵ_{tot} (%)	78.92	78.95	79.81	79.53
	Cost (yuan/kg)	0.02287	0.01874	0.02648	0.02031

5. Conclusion

The proposed steady state simulation of ARS chilling train system (from separation process in a typical ethylene plant) was validated successfully. Conventional exergy analysis was conducted to find the unit with highest exergy destruction. Then avoidable/unavoidable exergy destruction was calculated to identify the energy saving potential. In this system, DEP1 has the highest exergy destruction (1401.28 kW) and the highest rate of avoidable exergy destruction (89.04 %). Generally, reducing pressure drop and temperature difference can reduce the exergy destruction. Through the sensitivity analysis, effect of key variables on system exergy efficiency and operational cost can be obtained. By performing multi-objective optimisation aiming at maximizing system exergy efficiency and minimizing operational cost, the Pareto frontier is obtained, which can provide optimal solutions under different requirements.

The approach proposed in this study can also be used to improve other energy systems. The study indicates that there is still opportunity for energy efficiency improvements even for the well-developed processes. The findings from this study can guide the design and operation of separation process in ethylene manufacturing.

Nomenclature

Acronyms

ARS Advanced Recovery System

Sets

i Index of components

k Index of units

s Index of stages of DEPs

Parameters

Δt_{\min} Minimum temperature difference (°C)

$x_{i,k}^{ovhd,spec}$ Key components i mole fraction specification in overhead streams of columns k

$x_{i,k}^{btm,spec}$ Key components i mole fraction specification in bottom streams of columns k

$\omega_{ethylene}^{re}$ Coefficient of flowrate of ethylene refrigerant consumed in unit k to cost (yuan/kg)

$\omega_{propylene}^{re}$ Coefficient of flowrate of propylene refrigerant consumed in unit k to cost
(yuan/kg)

Continuous variables

T_{DEP1}^{ovhd} Temperature of the overhead stream of DEP1 (°C)

F_{DEP1}^{btm} Flowrate of the bottom stream of DEP1 (kg/h)

T_{DEP1}^{btm} Temperature of the bottom stream of DEP1 (°C)

T_{DEP2}^{ovhd} Temperature of the overhead stream of DEP2 (°C)

F_{DEP2}^{btm} Flowrate of the bottom stream of DEP2 (kg/h)

T_{DEP2}^{btm} Temperature of the bottom stream of DEP2 (°C)

T_{C1}^{ovhd} Temperature of the overhead stream of C1 (°C)

T_{C1}^{btm} Temperature of the bottom stream of C1 (°C)

F_{C1}^{btm} Flowrate of the bottom stream of C1 (kg/h)

T_{C1}^{sen} Temperature of the sensitive stage of C1 (°C)

T_{C3}^{ovhd} Temperature of the overhead stream of C3 (°C)

T_{C3}^{btm} Temperature of the bottom stream of C3 (°C)

$x_{C3}^{btm,ethylene}$ Mole fraction of ethylene of the bottom stream of C3

T_{C3}^{sen} Temperature of the sensitive stage of C3 (°C)

$T_{ME3}^{in,methane}$ Temperature of inlet methane stream of ME3 (°C)

$T_{ME3}^{out,cracked\ gas}$ Temperature of inlet cracked gas of ME3 (°C)

$T_{ME4}^{in,methane}$ Temperature of inlet methane stream of ME4 (°C)

$T_{ME4}^{out,cracked\ gas}$	Temperature of inlet cracked gas of ME4 (°C)
E^{ph}	Physical exergy (kW)
H	Enthalpy (kJ/kg)
S	Entropy (kJ/kg/K)
Z	Global composition of process stream
E^{ch}	Chemical exergy (kW)
x_i	Mole fraction of component i
R	Gas constant (8.31451 kJ/kmol/K)
e_i^0	Mole standard chemical exergy of the component i (kJ)
ΔG_f^0	Standard Gibbs energy of formation (J/mol)
n	Mole flowrate (mole/s)
$E_{F,tot}$	Exergy of the feed streams of system (kW)
$E_{P,tot}$	Exergy of the product streams of system (kW)
$E_{D,tot}$	Exergy destruction of system (kW)
$E_{L,tot}$	Exergy loss of system (kW)
$E_{D,k}$	Exergy destruction of unit k (kW)
$E_{F,k}$	Exergy of the feed stream of unit k (kW)
$E_{P,k}$	Exergy of the product stream of unit k (kW)
ε_k	Exergy efficiency of unit k (kW)
$E_{F,k}^{cold}$	Exergy of the cold feed stream of unit k (kW)
$E_{P,k}^{cold}$	Exergy of the cold product stream of unit k (kW)

$E_{F,k}^{hot}$	Exergy of the hot feed stream of unit k (kW)
$E_{P,k}^{hot}$	Exergy of the hot product stream of unit k (kW)
$E_{D,k}^{UN}$	Unavoidable exergy of unit k (kW)
$E_{D,k}^{AV}$	Avoidable exergy of unit k (kW)
α_i	Relative volatility of component i
$x_{feed,i}$	Mole fraction of component i of the feed stream of columns
θ	Parameter of the Underwood's method equation
q	The liquid fraction of the feed stream of columns
R_{min}	Minimum reflux ratio (mole)
$x_{ovhd,i}$	Mole fraction of component i of the overhead stream of columns
$E_{D,k}^{EN}$	Endogenous exergy destruction of unit k (kW)
$E_{D,k}^{EX}$	Exogenous exergy destruction of unit k (kW)
ΔT_{app}	Temperature approach ($^{\circ}\text{C}$)
ΔP	Pressure drop (kPa)
ΔP_{feed}	Pressure drop on the feed stage (kPa)
η_{is}	Isentropic efficiency (%)
$F_{stream103}$	Flowrate of heat exchange media in ME1 (Stream 103) (kg/h)
$F_{stream121}$	Flowrate of heat exchange media in ME2 (Stream 121) (kg/h)
$F_{stream154}$	Flowrate of heat exchange media in DEP1 (Stream 154) (kg/h)
$F_{stream155}$	Flowrate of heat exchange media in DEP1 (Stream 155) (kg/h)
$F_{stream167}$	Flowrate of heat exchange media in ME5 (Stream 167) (kg/h)

$Frac_{149}$	The split fraction of Stream 149
$F_{ethylene,k}^{re}$	Refrigerant ethylene consumption of unit k (kg/h)
$F_{propylene,k}^{re}$	Refrigerant propylene consumption of unit k (kg/h)
$F_{ethylene}^{pro}$	Flowrate of product ethylene (kg/h)
$T_{k,s}^{main}$	Main stream temperature on stage s of dephlegmator k (°C)
$T_{k,s}^{cold,in}$	Cold stream inlet temperature on stage s of dephlegmator k (°C)
$x_{i,k}^{ovhd}$	Key components i mole fraction in overhead streams of columns k
$x_{i,k}^{btm}$	Key components i mole fraction in bottom streams of columns k

Acknowledgements

The work was supported by the National Natural Science Foundation of China (Basic Science Center Program: 61988101), International (Regional) Cooperation and Exchange Project (61720106008), and the National Natural Science Fund for Distinguished Young Scholars (61725301, 61925305). The first author of this article would like to acknowledge the financial support from the China Scholarship Council (N0.201906740089).

References

- [1] Y. Chen., Y. Han., Q. Zhu, Appl. Therm. Eng. 119 (2017) 156–64. 10.1016/j.applthermaleng.2017.03.051.
- [2] C.A. Frangopoulos, Energy 164 (2018) 1011–20. 10.1016/j.energy.2018.08.218.
- [3] L. Zhao., F. You, Energy 182 (2019) 559–69. 10.1016/j.energy.2019.06.086.
- [4] F. Shen., X. Wang., L. Huang., Z. Ye., F. Qian, Ind. Eng. Chem. Res. 58(4) (2019) 1686–700. 10.1021/acs.iecr.8b05247.
- [5] F. Shen., L. Zhao., W. Du., W. Zhong., F. Qian, Appl. Energy 259 (2020) 114199. 10.1016/j.apenergy.2019.114199.
- [6] Stone & Webster International Projects Crop., Revamping of Separation Section of Ethylene Plant - Process Design Package, Vol. 1, 2000.
- [7] J. Zhang., Y. Wen., Q. Xu, Ind. Eng. Chem. Res. 49(12) (2010) 5786–99. 10.1021/ie100455g.

- [8] C. Xu, J. Zhang, H. Dinh, Q. Xu, *Ind. Eng. Chem. Res.* 56(28) (2017) 7984–99. 10.1021/acs.iecr.7b00111.
- [9] G.A. Lucadamo, D.P. Bernhard, H.C. Rowles, *Gas Sep. Purif.* 1(2) (1987) 94–102. 10.1016/0950-4214(87)80017-8.
- [10] L.M. Vane, F.R. Alvarez, A.P. Mairal, R.W. Baker, *Ind. Eng. Chem. Res.* 43(1) (2004) 173–83. 10.1021/ie0305667.
- [11] J. Wang, R. Smith, *Chem. Eng. Res. Des.* 83(9) (2005) 1133–44. 10.1205/cherd.04143.
- [12] Y. Casas, L.E. Arteaga, M. Morales, E. Rosa, L.M. Peralta, J. Dewulf, *Chem. Eng. J.* 162(3) (2010) 1057–66. 10.1016/j.cej.2010.06.021.
- [13] A.K. Olaleye, M. Wang, G. Kelsall, *Fuel* 151 (2015) 57–72. 10.1016/j.fuel.2015.01.013.
- [14] A.K. Olaleye, M. Wang, *Int. J. Greenh. Gas Control* 64 (2017) 246–56. 10.1016/j.ijggc.2017.08.002.
- [15] Y.-J. Lin, G.T. Rochelle, *Chem. Eng. J.* 283 (2016) 1033–43. 10.1016/j.cej.2015.08.086.
- [16] S. Bechtel, T. Vidakovic-Koch, K. Sundmacher, *Chem. Eng. J.* 346 (2018) 535–48. 10.1016/j.cej.2018.04.064.
- [17] M. Elhelw, K.S. Al Dahma, A. el H. Attia, *Appl. Therm. Eng.* 150 (2019) 285–93. 10.1016/j.applthermaleng.2019.01.003.
- [18] C. Yan, L. Lv, S. Wei, A. Eslamimanesh, W. Shen, *Appl. Therm. Eng.* 154 (2019) 637–49. 10.1016/j.applthermaleng.2019.03.128.
- [19] A. Malik, S.R. Qureshi, N. Abbas, A.A. Zaidi, *Sustain. Energy Technol. Assess.* 37 (2020) 100596. 10.1016/j.seta.2019.100596.
- [20] B. Wang, M. Pamminger, T. Wallner, *Appl. Energy* 254 (2019) 113645. 10.1016/j.apenergy.2019.113645.
- [21] B. Ma, A. Yao, C. Yao, T. Wu, B. Wang, J. Gao, C. Chen, *Appl. Energy* 261 (2020) 114483. 10.1016/j.apenergy.2019.114483.
- [22] F.M. Fábrega, J.S. Rossi, J.V.H. d’Angelo, *Energy* 35(3) (2010) 1224–31. 10.1016/j.energy.2009.11.001.
- [23] A. Ghannadzadeh, M. Sadeqzadeh, *J. Clean. Prod.* 129 (2016) 508–20. 10.1016/j.jclepro.2016.04.018.
- [24] F.S. Jahromi, M. Beheshti, R.F. Rajabi, *Energy* 164 (2018) 1114–34. 10.1016/j.energy.2018.09.059.
- [25] B. Yuan, Y. Zhang, W. Du, M. Wang, F. Qian, *Appl. Energy* 254 (2019) 113583. 10.1016/j.apenergy.2019.113583.
- [26] B. Ghorbani, R. Shirmohammadi, M. Mehrpooya, *Appl. Therm. Eng.* 132 (2018) 283–95. 10.1016/j.applthermaleng.2017.12.099.
- [27] M.M. Joybari, F. Haghghat, *Energy Convers. Manag.* 126 (2016) 799–810. 10.1016/j.enconman.2016.08.029.
- [28] D. Wu, B. Hu, R.Z. Wang, *Renew. Energy* 116 (2018) 775–85. 10.1016/j.renene.2017.10.024.
- [29] Z. Sun, Q. Wang, Z. Xie, S. Liu, D. Su, Q. Cui, *Energy* 170 (2019) 1170–80. 10.1016/j.energy.2018.12.055.
- [30] W. Chen, Z. Li, Q. Sun, B. Zhang, *Energy Convers. Manag.* 191 (2019) 55–70. 10.1016/j.enconman.2019.04.024.
- [31] A. Razmi, M. Soltani, M. Torabi, *Energy Convers. Manag.* 195 (2019) 1199–211. 10.1016/j.enconman.2019.05.065.
- [32] J.U. Ahamed, R. Saidur, H.H. Masjuki, *Renew. Sustain. Energy Rev.* 15(3) (2011) 1593–600. 10.1016/j.rser.2010.11.039.
- [33] T. Morosuk, G. Tsatsaronis, *Energy* 33(6) (2008) 890–907. 10.1016/j.energy.2007.09.012.
- [34] Z. Wei, B. Zhang, S. Wu, Q. Chen, G. Tsatsaronis, *Energy* 42(1) (2012) 424–33. 10.1016/j.energy.2012.03.026.
- [35] G.D. Vučković, M.M. Stojiljković, M.V. Vukić, G.M. Stefanović, E.M. Dedeić, *Energy Convers. Manag.* 85 (2014) 655–62. 10.1016/j.enconman.2014.03.049.
- [36] M. Mehrpooya, R. Lazemzade, M.S. Sadaghiani, H. Parishani, *Energy Convers. Manag.* 123 (2016) 523–34. 10.1016/j.enconman.2016.06.069.
- [37] M. Penkuhn, G. Tsatsaronis, *Energy* 137 (2017) 854–64. 10.1016/j.energy.2017.02.175.
- [38] M. Mehdizadeh-Fard, F. Pourfayaz, M. Mehrpooya, A. Kasaeian, *Appl. Therm. Eng.* 137 (2018) 341–55. 10.1016/j.applthermaleng.2018.03.054.
- [39] Z. Mohammadi, M. Fallah, S.M.S. Mahmoudi, *Energy* 178 (2019) 631–43. 10.1016/j.energy.2019.04.134.

- [40] E. Gholamian,, P. Hanafizadeh,, P. Ahmadi, *Appl. Therm. Eng.* 137 (2018) 689–99. 10.1016/j.applthermaleng.2018.03.055.
- [41] M. Yu,, Z. Chen,, D. Yao,, F. Zhao,, X. Pan,, X. Liu,, P. Cui,, Z. Zhu,, Y. Wang, *Energy Convers. Manag.* 221 (2020) 113162. 10.1016/j.enconman.2020.113162.
- [42] P. Cui,, M. Yu,, Z. Liu,, Z. Zhu,, S. Yang, *Energy Convers. Manag.* 184 (2019) 249–61. 10.1016/j.enconman.2019.01.047.
- [43] A.G. Kaviri,, M.N.Mohd. Jaafar,, T.M. Lazim, *Energy Convers. Manag.* 58 (2012) 94–103. 10.1016/j.enconman.2012.01.002.
- [44] M. Di Somma,, B. Yan,, N. Bianco,, G. Graditi,, P.B. Luh,, L. Mongibello,, V. Naso, *Appl. Energy* 204 (2017) 1299–316. 10.1016/j.apenergy.2017.03.105.
- [45] C. Qin,, Q. Yan,, G. He, *Energy* 188 (2019) 116044. 10.1016/j.energy.2019.116044.
- [46] Aspen Technology, Inc., ASPEN PLUS® Aspen Plus User Guide Version 8.4, 2013.
- [47] J. Szargut,, D.R. Morris,, F.R. Steward, *Exergy analysis of thermal, chemical, and metallurgical processes*, Hemisphere Publishing, New York, NY, United States, 1987.
- [48] A. Ghannadzadeh,, R. Thery-Hetrex,, O. Baudouin,, P. Baudet,, P. Floquet,, X. Joulia, *Energy* 44(1) (2012) 38–59. 10.1016/j.energy.2012.02.017.
- [49] J. Ahrendts, *Energy* 5(8–9) (1980) 666–77. 10.1016/0360-5442(80)90087-0.
- [50] A. Lazzaretto,, G. Tsatsaronis, *Energy* 31(8–9) (2006) 1257–89. 10.1016/j.energy.2005.03.011.
- [51] G. Tsatsaronis, in: A. Bejan, E. Mamut (Eds.), *Thermodynamic Optimization of Complex Energy Systems*, Springer Netherlands, Dordrecht, 1999, pp. 93–100.
- [52] Y. Yang,, L. Wang,, C. Dong,, G. Xu,, T. Morosuk,, G. Tsatsaronis, *Appl. Energy* 112 (2013) 1087–99. 10.1016/j.apenergy.2012.12.063.
- [53] T. Morosuk,, G. Tsatsaronis, *Energy* 33(6) (2008) 890–907. 10.1016/j.energy.2007.09.012.
- [54] M.M.- Fard,, F. Pourfayaz, *J. Clean. Prod.* 206 (2019) 670–87. 10.1016/j.jclepro.2018.09.166.
- [55] M. Mehrpooya,, R. Lazemzade,, M.S. Sadaghiani,, H. Parishani, *Energy Convers. Manag.* 123 (2016) 523–34. 10.1016/j.enconman.2016.06.069.
- [56] Y. del Valle,, G.K. Venayagamoorthy,, S. Mohagheghi,, J.-C. Hernandez,, R.G. Harley, *IEEE Trans. Evol. Comput.* 12(2) (2008) 171–95. 10.1109/TEVC.2007.896686.
- [57] H. Sayyaadi,, M. Nejatollahi, *Int. J. Refrig.* 34(1) (2011) 243–56. 10.1016/j.ijrefrig.2010.07.026.